

PACS numbers: 42.81.Cn; 42.81.Dp; 42.81.Uv; 42.55.Wd
DOI: 10.1070/QE2012v042n09ABEH014970

Bismuth-doped optical fibres: A new breakthrough in near-IR lasing media

E.M. Dianov

Abstract. **Recent results demonstrate that bismuth-doped optical fibres have considerable potential as near-IR active lasing media. This paper examines bismuth-doped fibres intended for the fabrication of fibre lasers and optical amplifiers and reviews recent results on the luminescence properties of various types of bismuth-doped fibres and the performance of bismuth-doped fibre lasers and optical amplifiers for the spectral range 1150–1550 nm. Problems are discussed that have yet to be solved in order to improve the efficiency of the bismuth lasers and optical amplifiers.**

Keywords: *fibre laser, fibre amplifier, bismuth-doped optical fibres, optical fibre communication.*

1. Introduction

After the first laser was demonstrated in 1960, a great deal of attention was paid to the search for and fabrication of novel active lasing media, which made it possible to improve the performance of existing lasers and create new ones. This area of modern materials research continues to attract great interest because there is a constant need for novel lasers and optical amplifiers for many applications, in particular for the next generation of optical fibre communication systems. Modern commercial optical fibre systems have per-fibre capacities of up to 10 Tbit s^{-1}, and the data rate in pilot systems has reached ~100 Tbit s^{-1} [1]. This is a tremendous success in the development of optical fibre communication and information transfer systems, but the need for information in the developed countries increases by 30% to 40% every year. This means that, in twenty years, there will be a need for data transmission at petabit rates. A number of approaches to this problem have been discussed in the literature (see, e.g., Ref. [2]). One possibility is to extend the spectral range of data transmission. Modern high-speed optical fibre communication networks employ only a narrow (80 nm) spectral range, 1530–1610 nm, defined by the gain band of the erbium-doped fibre amplifier. At the same time, as seen in Fig. 1 silica-based fibres have low optical losses in a considerably broader range. In particular, the spectral region where the optical loss is under 0.4 dB km^{-1} and which might be used for data transmission is 400 nm in width (1300–1700 nm).

E.M. Dianov Fiber Optics Research Center, Russian Academy of Sciences, ul. Vavilova 38, 119333 Moscow, Russia;
e-mail: dianov@fo.gpi.ru

Received 28 August 2012
Kvantovaya Elektronika **42** (9) 754–761 (2012)
Translated by O.M. Tsarev

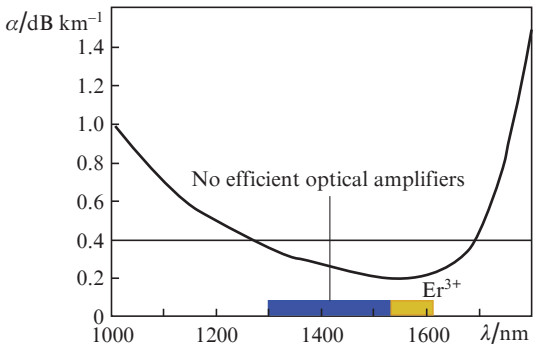

Figure 1. Optical loss spectrum of silica-based fibres and spectral region where the erbium-doped fibre amplifier operates (Er^{3+}) and which is currently employed for high-speed data transmission.

At present, however, efficient fibre amplifiers – necessary components of high-speed optical fibre communication and information transfer systems – for the spectral ranges 1300–1520 and 1610–1700 nm are missing. The most efficient active media for the near-IR spectral region are rare-earth-doped fibres. Unfortunately, their luminescence bands are unsuitable for creating efficient optical amplifiers in the above spectral ranges. In connection with this, there is an urgent need for new active optical materials suitable for creating efficient fibre lasers and optical amplifiers operating at the wavelengths in question. Attempts to develop efficient active materials doped with transition metals have been unsuccessful.

As found in 2001, bismuth-doped aluminosilicate glass photolumineses in a broad spectral region (1000–1600 nm) with luminescence bands 200–300 nm in width [3]. This finding attracted great interest and led to a number of studies concerned with luminescence in bismuth-doped glasses of various compositions. The interest in such glasses increased sharply after the first demonstration of lasing in a bismuth-doped fibre [4].

During the decade after the discovery of near-IR luminescence in bismuth-doped silica glass, many reports focused on such luminescence in various bismuth-doped glasses and crystals. The luminescence of bismuth centres has been observed and investigated in silicate, germanate, aluminoborate, aluminosilicate, aluminophosphate, borosilicate and chalcogenide glasses in the spectral range 1000–2000 nm (see e.g. reviews by Peng et al. [5] and Dianov [6]). Despite the large number of reports concerned with the IR luminescence of bismuth in glasses, the nature of the IR-emitting Bi centres in glasses is not yet clear [5, 6]. This is a serious obstacle to creating efficient active media based on bismuth-doped glasses. It

is not by chance that no lasing has been demonstrated to date in bismuth-doped bulk glasses.

This paper summarises the results of research aimed at producing various bismuth-doped fibres and investigating their luminescence properties and presents recent data on the performance of bismuth-doped fibre lasers that employ already existing fibres.

The Conclusions section formulates the problems encountered in creating highly efficient bismuth-doped fibre lasers and optical amplifiers and highlights the basic research directions that offer promise of solving these problems.

2. Bismuth-doped glass fibres and their luminescence properties

The first bismuth-doped optical fibres were fabricated simultaneously and independently at the Fiber Optics Research Center (FORC), Russian Academy of Sciences (RAS) in cooperation with the Institute of Chemistry of High-Purity Substances, RAS [7] and at Sumitomo Electric Industries, Ltd (Japan) [8] in 2005.

The bismuth-doped fibre was fabricated using modified chemical vapour deposition (MCVD), a process widely employed to produce standard optical fibres (see e.g. Ref. [9]). The fibre core consisted of bismuth–aluminium codoped silica glass that had been the first to exhibit near-IR luminescence [3]. In addition, Dvoyrin et al. [7] fabricated a bismuth-doped phosphogermanosilicate fibre in order to assess the influence of glass composition on the luminescence properties of the fibres. The core glasses in the fibres had the following compositions (mol %):

$$0.03Bi_2O_3-10Al_2O_3-90SiO_2 \text{ (fibre A)},$$

$$0.002Bi_2O_3-1Al_2O_3-2P_2O_5-9GeO_2-88SiO_2 \text{ (fibre G)}.$$

The fibres had a pure silica cladding. Figure 2 shows the luminescence spectra of the fibres at an excitation wavelength $\lambda_p = 676$ nm. The spectra are similar to the luminescence spectrum of the bismuth–aluminium doped silica glass prepared by Fujimoto and Nakatsuka [3]. At an excitation wavelength $\lambda_p = 1064$ nm, the luminescence lifetime was 800 and 1200 μs in fibres G and A, respectively. The optical loss spectrum of fibre A is presented in Fig. 3.

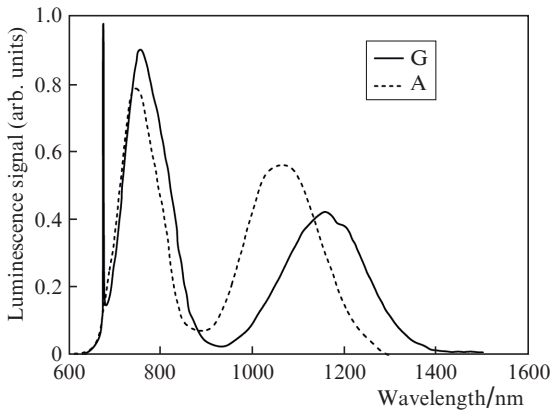

Figure 2. Luminescence spectra of the first bismuth-doped optical fibres.

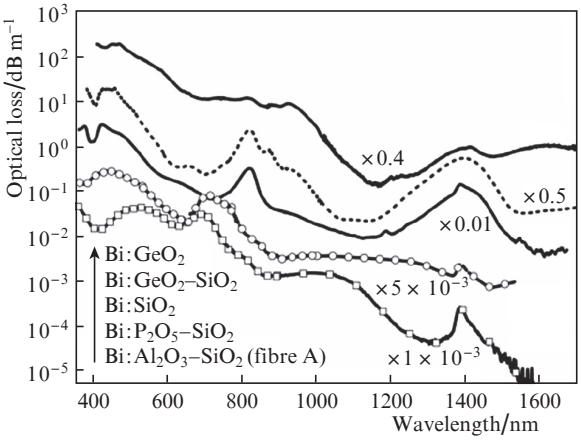

Figure 3. Optical loss spectra of various bismuth-doped optical fibres. The numbers at the spectra specify the degree of compression of the vertical scale for convenience of comparison. The fibre compositions vary from the bottom spectrum to the upper spectra.

Later, other types of bismuth-doped fibres were proposed, with Bi:SiO_2, Bi:GeO_2, Bi:SiO_2–GeO_2, Bi:SiO_2–P_2O_5, and Bi:SiO_2–GeO_2–P_2O_5 glass cores.

Fibre preforms with a silica core (standard and microstructured) were fabricated by different methods: MCVD [11], powder-in-tube process [10] and sol–gel processing [46]. The other preforms were fabricated by MCVD [10, 11]. All the fibres were drawn from preforms under identical conditions: heating to about 2000 °C followed by rapid cooling of the fibre during drawing to below the glass transition temperature in a time shorter than 1 s. The bismuth concentration in the fibre core was no higher than the detection limit of our analytical equipment and was estimated at under 0.02 at %. The results of early studies of the transmission (absorption) and luminescence spectra of various bismuth-doped fibres were presented in a number of reports and reviews (see e.g. Refs [12–16]).

Figure 3 shows the optical loss spectra of the above-mentioned fibres. All the spectra contain several broad absorption bands in the visible and near-IR spectral regions, which significantly facilitates pumping of bismuth-doped fibre lasers. The bottom spectrum is for the aluminosilicate fibre A, the first proposed and best studied bismuth-doped fibre. It contains well-known absorption bands centred at λ = 500, 700, 800, 1000 and 1400 nm. The absorption spectra are seen to depend on core glass composition. The fibres with silica and germanosilicate cores have similar absorption spectra.

Before discussing the luminescence properties of the above-mentioned fibres, I would like to make the following digression: As a rule, the luminescence spectra of bismuth-doped glasses and fibres are measured in a limited spectral range at particular excitation wavelengths. Such measurements are incapable of providing a complete picture of the luminescence of the samples, necessary for adequate interpretation of their spectra. In our studies, the luminescence intensity I_{lum} of bismuth-doped fibres was measured as a function of excitation wavelength (λ_{ex}) and emission wavelength (λ_{em}) in a wide spectral region (450–1700 nm). Luminescence excitation at various wavelengths was ensured by an SC450 supercontinuum source (Fianium). Narrow-band radiation ($\Delta\lambda$ = 3 nm) was selected by an acousto-optic filter and launched into the fibre core. Luminescence spectra were taken

with an HP spectrum analyser in the range 875 nm $< \lambda_{em} <$ 1700 nm and with an SP200 spectrometer (Ocean Optics) in the range 450 nm $< \lambda_{em} <$ 875 nm. In this way, we obtained luminescence spectra at λ_{ex} varied from 450 to 1700 nm in 10-nm steps.

The luminescence spectra were corrected for the spectral sensitivity of the measuring channel and normalised to the launched pump power. Such measurements allowed us to construct $I_{lum}(\lambda_{ex}, \lambda_{em})$ contour plots for optical fibres with $Bi:SiO_2$, $Bi:GeO_2$, $Bi:P_2O_5–SiO_2$ and $Bi:Al_2O_3–SiO_2$ cores (Fig. 4) [17]. In Fig. 4, the ratio of the highest to the lowest luminescence intensity is ~100. This restricts regions with low luminescence intensities, otherwise the graphs would be difficult to use in analysis of the energy level structure of bismuth centres. In other words, the three-dimensional graphs in Fig. 4 represent only the main, brightest luminescence peaks. As seen in Fig. 4, the luminescence spectra of all the fibres consist of composite peaks, many of which overlap. All the $I_{lum}(\lambda_{ex}, \lambda_{em})$ graphs contain a line along the $\lambda_{ex} = \lambda_{em}$ diagonal, due to the scattered excitation light.

The luminescence spectrum of the silica core fibre has the simplest form (Fig. 4a). There is a red luminescence band centred at 590 nm, due to Bi^{2+}. The origin of the red luminescence was discussed in detail by Firstov et al. [17]. The IR luminescence spectrum consists of two bands: one centred at λ_{em} = 830 nm and excited at λ_{ex} = 420 and 820 nm, and the other centred at 1430 nm and excited at λ_{ex} = 420, 820 and 1420 nm. In what follows, we assign these bands to bismuth in the silica glass.

Figure 4b shows the luminescence spectrum of the germanate core fibre. Surprisingly enough, the red luminescence due to Bi^{2+} is missing. There is still no reliable interpretation of this fact. The luminescence bands at λ_{em} = 830 and 1430 nm are due to the small percentage of silica glass in the germanate core. The bismuth luminescence spectrum shows two new bands, at 950 and 1650 nm. In what follows, we assign these bands to bismuth in the germanate glass.

Figure 4c shows the luminescence picture of the phosphosilicate fibre. The luminescence band centred at 750 nm and excited at 520 nm is due to Bi^{2+}. There are also bands at λ_{em} = 830 and 1430 nm, due to silica glass. The broad luminescence bands in the range 1100–1300 nm are due to phosphorus. The luminescence spectrum of the aluminosilicate core fibre is presented in Fig. 4d. The luminescence band at λ_{em} = 750 nm is due to Bi^{2+}, the 830-nm band arises from bismuth in silica glass, and the three broad luminescence bands in the range 1000–1250 nm correspond to aluminium.

Figure 5 summarises the luminescence measurement results for the optical fibres studied. Taking into account the luminescence bandwidths (100 nm or more), we conclude that the

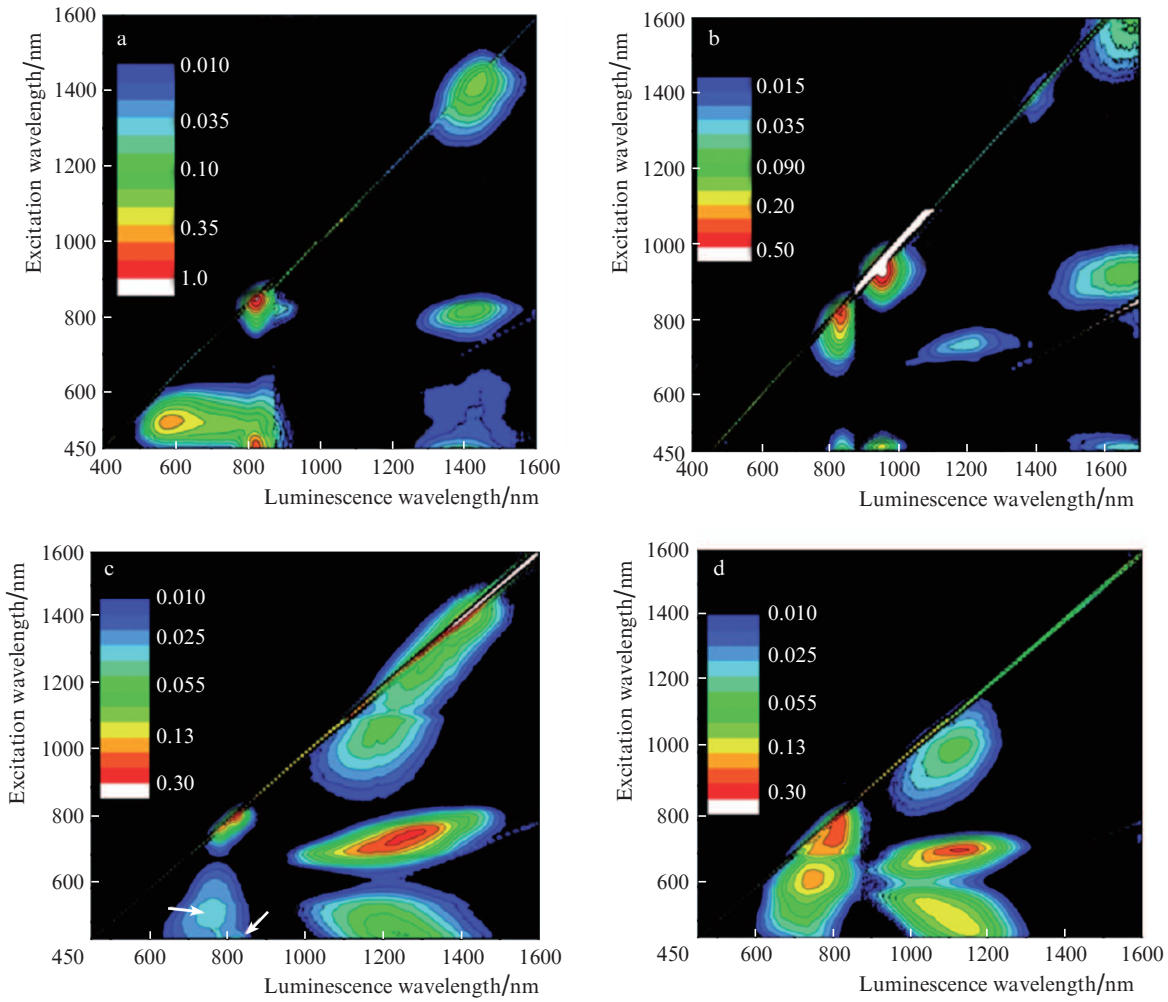

Figure 4. Luminescence intensity contour plots for bismuth-doped fibres: (a) $Bi:SiO_2$, (b) $Bi:GeO_2$, (c) $Bi:P_2O_5–SiO_2$ and (d) $Bi:Al_2O_3–SiO_2$ fibres.

luminescence of the bismuth centres in the fibres studied covers the entire spectral range 800–1700 nm. Also indicated in Fig. 5 are the luminescence lifetimes for various bands. At wavelengths of 1000 nm and longer, the luminescence lifetime lies in the range 600–1000 μs; at shorter wavelengths, the lifetime ranges from 3 to 50 μs. The luminescence properties of bismuth-doped fibres were discussed in detail by Firstov et al. [17].

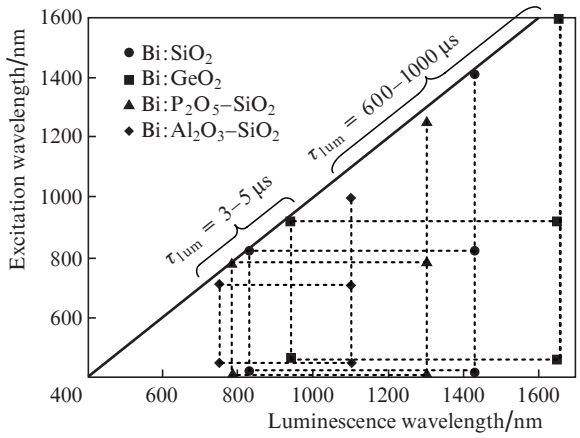

Figure 5. Sum diagram of the major luminescence peaks of various bismuth-doped optical fibres.

3. Bismuth-doped fibre lasers

It follows from the above luminescence data (spectra and lifetime) that, in the fibres under consideration, lasing can be achieved over the entire spectral range 800–1700 nm. An extremely important point is the possibility of producing fibre lasers and optical amplifiers in the range 1300–1500 nm, potentially attractive for information transfer through next-generation optical fibre communication systems.

The first bismuth-doped solid-state (fibre) laser was produced at FORC in 2005 [4]. The gain medium used was an aluminosilicate fibre – one of the first bismuth-doped fibres obtained [7]. Figure 4d suggests the possibility of lasing in such fibre in the spectral range 1000–1250 nm. There is great interest in lasers for this spectral region, especially for the range 1150–1250 nm, which contains no rare-earth lasing wavelengths. The design of the bismuth-doped fibre laser was typical of fibre lasers with a cavity formed by fibre Bragg gratings. The 1060-nm pump light from a neodymium fibre laser was coupled directly into the core of the active fibre. CW lasing with an efficiency of ~10% was achieved in the spectral range 1150–1215 nm.

The demonstration of the first bismuth-doped fibre laser initiated active development and investigation of such lasers. A number of bismuth lasers were made using aluminosilicate fibres, including cw lasers with a higher efficiency [14, 15, 18–20], picosecond lasers [21–26] and narrow-band lasers for second harmonic generation [16, 18, 19, 28]. Note that the frequency-doubled, yellow radiation (575–590 nm) of bismuth-doped aluminosilicate fibre lasers is of interest for medical applications, including dermatology [29] and ophthalmology [30]. Of particular interest is the direct generation of 589-nm radiation through second harmonic generation with a bismuth laser in order to create a guide star for astronomical applications [31].

Yet another application of bismuth-doped aluminosilicate fibre lasers is related to the development of Q-switched all-fibre lasers. One problem in creating such lasers is to select an appropriate saturable fibre absorber. A bismuth-doped aluminosilicate fibre with an absorption band near 1000 nm, covering the lasing region of Yb lasers, could be employed as such an absorber for the widely used Yb-doped fibre laser. However, the excited state lifetime of Bi is ~800 μs, which limits the pulse repetition rate by an unacceptably low value (~1 kHz). To overcome this limitation, Dvoyrin et al. [32] proposed a configuration in which a bismuth-doped fibre was placed in a separate cavity in order to reduce the excited state lifetime of the bismuth. The Yb–Bi fibre laser configuration is shown in Fig. 6. Pulsed lasing was obtained in the range 1050–1215 nm (in both lasers), and the repetition rate of ~1-μs pulses was up to 100 kHz.

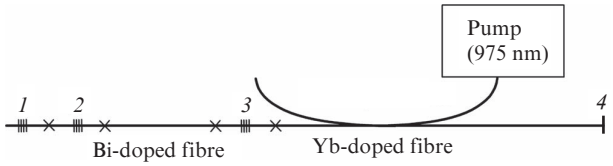

Figure 6. Bismuth-doped fibre laser placed in the cavity of an Yb-doped fibre laser and used as a saturable absorber of a Q-switched Yb laser: (*1*, *2*) highly reflective fibre Bragg gratings, (*4*, *3*) output couplers of the Yb and Bi lasers, respectively.

A number of detailed studies [18–20, 27, 33] focused on the influence of parameters of active aluminosilicate fibres – with emphasis on the pump and lasing wavelengths and bismuth concentration – on the bismuth laser efficiency. A large fraction of nonsaturable absorption was found at the pump wavelength λ_p. The absorption depended on λ_p and increased with increasing bismuth concentration. An increase in bismuth concentration led to clustering of bismuth-related active centres, as was evidenced by a nonexponential luminescence decay at relatively high bismuth concentrations. Moreover, evidence was found for absorption from an excited state of the bismuth and cooperative effects resulting, in particular, in visible emission (540 nm) under IR pumping. All these phenomena limit the efficiency of bismuth lasers, so that very low bismuth concentrations (of the order of 0.01 at %) have to be used in order to improve lasing efficiency. Low concentrations are a drawback to this laser system because they require long lengths (50–100 m) of active fibres and make cladding pumping of fibre lasers impossible. It may be that this drawback will be eliminated when the nature of the bismuth-related active centres in glasses will be better understood. Note in passing that it is the necessity of using very low bismuth concentrations for efficient lasing which accounts for the failure of attempts to achieve lasing in bulk bismuth-doped glasses.

An inherent drawback to Bi-doped aluminosilicate fibre lasers is the narrow spectral range of their lasing. To date, lasing has been achieved in the range 1150–1215 nm. At a pump wavelength λ_p = 1070 nm, the laser efficiency at 1150 and 1160 nm was 19% and 21%, and the output power was 13 and 15 W, respectively. At wavelengths of 1205 and 1215 nm, the

efficiency was ~7% [18]. The highest efficiency, 28%, was reached at 1179 nm under pumping at 1090 nm [20].

Bismuth-doped fibre lasers and optical amplifiers for longer wavelengths (over 1250 nm) were made using phosphogermanosilicate [34–36] and germanosilicate [37–40] fibres, as well as silica core fibres [11, 41]. Given below are the results on the performance of two high-power cw lasers operating at 1270 and 1460 nm and a bismuth-doped fibre amplifier with a peak gain at 1460 nm.

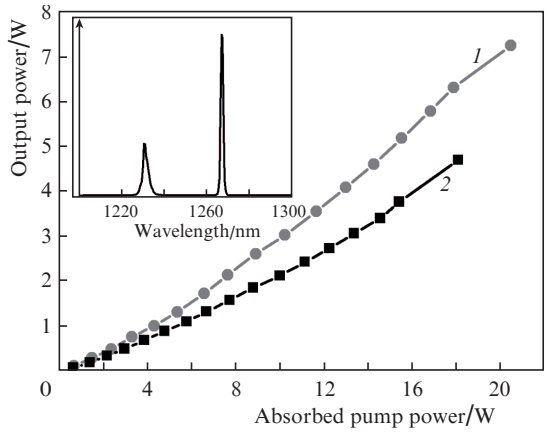

Figure 7. Output laser power at 1268 nm as a function of absorbed pump power at output coupler reflectances of (*1*) 50% and (*2*) 25%. Inset: laser emission spectrum.

A fibre laser emitting at 1270 nm is of interest for many applications, in particular for medicine [42], and its second harmonic is capable of competing with the He–Ne laser. The laser design was typical of cw fibre lasers: use was made of a 95-m length of bismuth-doped phosphogermanosilicate fibre and two fibre Bragg gratings fusion-spliced to the ends of the bismuth-doped fibre [36]. The reflectance of one grating was about 100%. As the output coupler, we used a 50% or 25% reflective grating. The spectral bandwidth of all the Bragg gratings was 0.5 nm. The pump source used was a Raman fibre laser emitting at 1230 nm with an output power of up to 25 W. Figure 7 shows the output power of the bismuth laser as a function of absorbed pump power. CW lasing at 1268 nm with a 7-W power and 35% efficiency has been achieved for the first time.

The bismuth-doped phosphogermanosilicate fibre was also used to produce an optical amplifier operating in a spectral region around 1300 nm. At a pump wavelength of 1230 nm and pump power of 460 mW, the gain had a 25-dB maximum at 1320 nm, with a bandwidth of 40 nm [35].

Another new result is the development of high-power, efficient bismuth-doped fibre lasers emitting in the spectral range 1390–1530 nm [37–39]. The gain medium of these lasers was a germanosilicate fibre containing no more than 0.01 at % Bi. The fibre length was 95 m, which ensured an almost complete pump absorption. The luminescence band of the fibre had a 3-dB width of ~150 nm, with a peak emission wavelength near 1430 nm.

Figure 8 shows the configuration of a laser emitting at 1460 nm. The pump source used (λ_p = 1340 nm) was a phosphosilicate fibre Raman laser, which was in turn pumped by an Yb-doped fibre laser at 1137 nm. Figure 9a shows the output power of the bismuth laser as a function of pump power. The highest output power was 22 W, and the pump efficiency was 50%.

Figure 9b shows the temperature dependences of efficiency for bismuth-doped aluminosilicate, phosphogermanosilicate and germanosilicate fibre lasers. The efficiency of the bismuth-doped germanosilicate fibre laser is seen to be a weak function of temperature.

The broad luminescence band of the bismuth-doped germanosilicate fibre, with a peak emission wavelength near 1430 nm, suggests that lasing can be achieved at various wavelengths within this band. To verify this possibility, we used several laser configurations in which grating pairs for wavelengths between 1389 and 1538 nm were placed instead of the fibre Bragg gratings in Fig. 8. Lasing with several watts of output power and 30% to 65% efficiency was achieved at 1390, 1480, 1150 and 1538 nm [39]. Thus, the first bismuth-doped germanosilicate fibre laser with an output power above 20 W and 50% efficiency at 1460 nm has been demonstrated. Its efficiency decreases only slightly with increasing temperature. Lasing in the spectral range 1390–1540 nm showed rather high efficiency.

The bismuth-doped germanosilicate fibre was used to produce an efficient optical amplifier with a peak gain wavelength near 1430 nm. When pumped at λ_p = 1310 nm by a

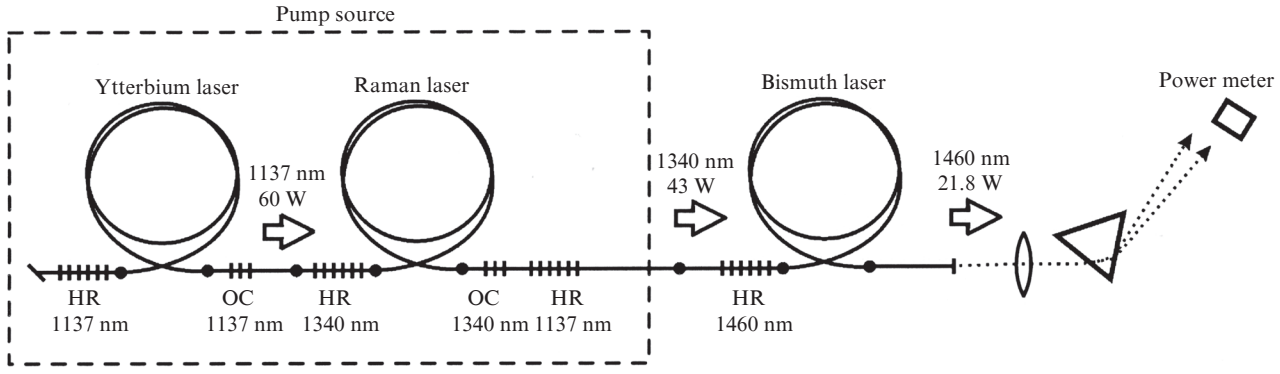

Figure 8. Configuration of a bismuth-doped fibre laser emitting at 1460 nm, with the positions and resonance wavelengths of the Bragg gratings that form the cavities of the pump lasers and bismuth laser; (HR) ~100% reflective Bragg gratings, (OC) Bragg gratings used as the output couplers of the lasers.

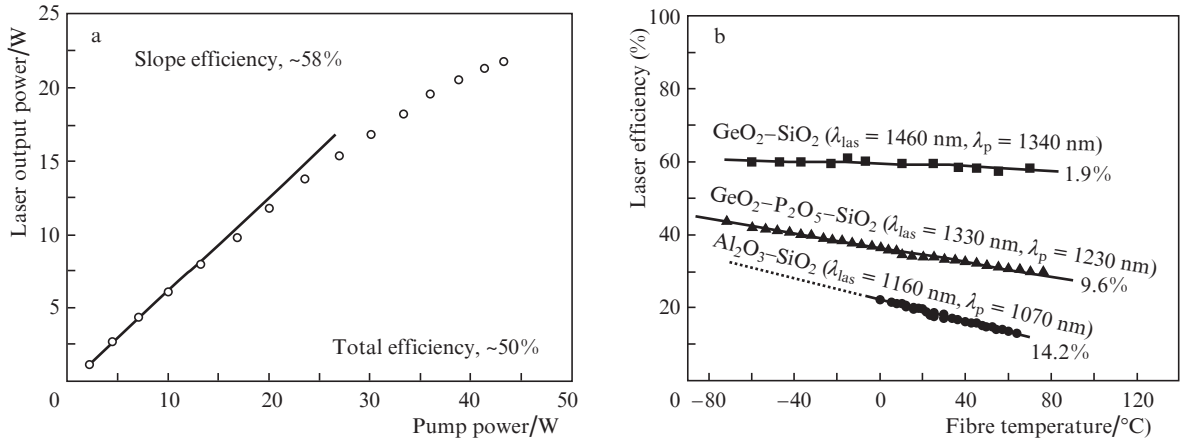

Figure 9. (a) Output power of a bismuth laser as a function of pump power at λ = 1340 nm. (b) Laser efficiency as a function of fibre temperature for various bismuth lasers (with the fibre core compositions, lasing and pump wavelengths and the percent reduction in efficiency on heating by 100 °C).

commercial 65-mW laser diode, it showed a gain of up to 25 dB. The 3-dB width of its gain band reached 40 nm, and its noise figure was 6 dB [40].

Figure 10 indicates the lasing wavelengths and maximum output powers of the cw bismuth-doped fibre lasers developed to date. The dots on the horizontal axis indicate the pump wavelengths and the corresponding lasing wavelengths (the wavelengths of the lasers with an output power under 1 W are not indicated). Thus, the bismuth-doped fibre lasers developed to date cover almost the entire spectral range 1150–1550 nm.

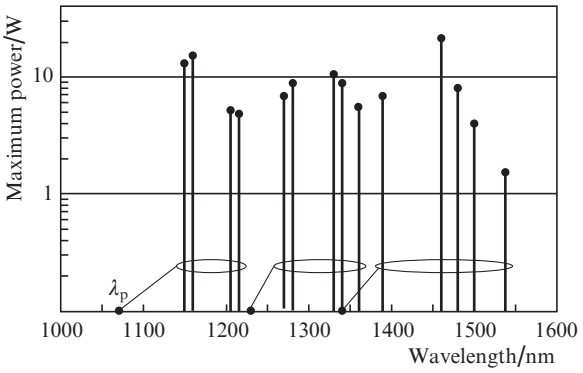

Figure 10. Output powers of various cw bismuth lasers operating in the spectral range 1150–1550 nm.

4. Conclusions

The results obtained so far confirm that bismuth-doped glass fibres have great potential as near-IR lasing media. The luminescence spectra of various bismuth-doped glasses cover the entire spectral range 800–2000 nm and have luminescence bands 150–300 nm in width.

A process has been developed for the fabrication of bismuth-doped optical fibres, which have been used to produce a family of bismuth-doped fibre lasers that have an efficiency from 25% to 50% and cover the spectral range 1150–1550 nm. An important point is that this range includes the spectral region 1300–1500 nm, which contains no wavelengths of efficient rare-earth lasers but is of importance in a number of applications, primarily in optical fibre communication. It is for this spectral region that bismuth-doped optical amplifiers with a gain of up to 25 dB at 1320 and 1430 nm and a gain band ~40 nm wide have been developed.

There are, however, a number of unresolved problems, natural when new laser materials are used. We mention only three of them.

1. Efficient operation of bismuth-doped fibre lasers has been achieved only at very low bismuth concentrations (no higher than 0.01 at %).

2. The efficiency of bismuth-doped fibre lasers and optical amplifiers reached to date is lower than that of their rare-earth-doped analogues.

3. The possible operation range of bismuth lasers, 800–2000 nm, has been covered only partly.

The difficulties in solving these problems are associated to a considerable extent with the distinctive features of bismuth as an active element.

First, in the preparation of bismuth-containing glasses use is made of starting compounds containing trivalent bismuth (Bi^{3+}), e.g. bismuth oxide, Bi_2O_3. In the glass preparation or fibre fabrication process, however, bismuth is reduced to a lower valence state at temperatures above 1000 °C. Only after this is the formation of near-IR emitting bismuth centres possible.

Second, a special feature of bismuth as a chemical element is that, with an increase in the melting point of glasses, it is reduced at an extremely high rate to form lower valence ions and various complexes [43, 44]:

$$Bi^{3+} \rightarrow Bi^{2+} \rightarrow Bi^{+} \rightarrow Bi \rightarrow \text{Bi clusters } (Bi_2, Bi_2^-, Bi_3 \ldots)$$

$$\rightarrow (Bi)_n \text{ colloids.}$$

The rate of this process depends on the temperature, glass composition, atmosphere and bismuth concentration.

The exact nature of the near-IR emitting bismuth centres is still unclear. There are a number of hypotheses as to the

origin of the IR luminescence, which has variously been assigned to Bi^+, Bi clusters, BiO, Bi_2^-, Bi_2^{2-}, point defects and other species, but none of them has been confirmed directly [5]. I believe that this luminescence originates not from an individual bismuth ion in a low-valence state but from defect centres consisting of a Bi ion in a low-valence state and a structural defect of the glass, most likely an anion (oxygen) vacancy [6, 45]. Further fundamental studies are needed to assess the nature of the near-IR emitting bismuth centres. But even if we will know their structure, we will have to face another problem: control over the reduction of Bi^{3+} in order to obtain Bi in the desired valence state, without excessive reduction of bismuth, which otherwise might lead to the formation of metallic bismuth clusters, the associated increase in the optical loss in the fibre and the other problems discussed in the preceding section. In other words, fundamental studies of the reduction of bismuth in glasses and the redox equilibrium of Bi in glasses are needed.

In the case of bismuth-doped silica fibres, such fundamental studies face serious difficulties because of the high temperatures, up to 2000 °C, used in the fibre fabrication process. At the same time, the above problems will be difficult to solve without such studies.

Acknowledgements. I am grateful to V.G. Plotnichenko and V.O. Sokolov (FORC) for useful discussions in preparing the manuscript and for their helpful comments.

References

1. *Proc. OFC Conf.* (Los Angeles, 2012).
2. Morioka Toshio. *Proc. Optoelectron. and Commun. Conf.* (Hong Kong, 2009) paper FT4.
3. Fujimoto Y., Nakatsuka M. *Jpn. J. Appl. Phys.*, **40**, L279 (2001).
4. Dianov E.M., Dvoyrin V.V., Mashinskii V.M., Umnikov A.A., Yashkov M.V., Gur'yanov A.N. *Kvantovaya Elektron.*, **35**, 1083 (2005) [*Quantum Electron.*, **35**, 1083 (2005)].
5. Peng M., Dong G., Wondraczek L., Zhang L., Zhang N., Qiu J. *J. Non-Cryst. Solids*, **357**, 2241 (2011).
6. Dianov E.M. *Light: Science and Applications*; 1, e12; doi:10.1038/lsa.2012.12 (2012).
7. Dvoyrin V.V., Mashinsky V.M., Dianov E.M., Umnikov A.A., Yashkov M.V., Guryanov A.N. *Proc. ECOC* (Glasgow, 2005) paper Th. 3.3.5.
8. Haruna T., Kakui M., Taru T., Ishikawa Sh., Onishi M. *Proc. Opt. Ampl. Appl. Topical Meeting* (Budapest, 2005) paper MC3.
9. Dianov E.M., Prokhorov A.M. *Usp. Fiz. Nauk*, **148**, 289 (1986).
10. Bufetov I.A., Semenov S.L., Vel'miskin V.V., Firstov S.V., Bufetova G.A., Dianov E.M. *Kvantovaya Elektron.*, **40**, 639 (2010) [*Quantum Electron.*, **40**, 639 (2010)].
11. Zlenko A.S., Dvoyrin V.V., Mashinsky V.M., Denisov A.N., Iskhakova L.D., Mayorova M.S., Medvedkov O.I., Semenov S.L., Vasiliev S.A., Dianov E.M. *Opt. Lett.*, **36**, 2599 (2011).
12. Dianov E.M. *Proc. SPIE Int. Soc. Opt. Eng.*, **6890**, 6890H-1 (2008).
13. Bufetov I.A., Dianov E.M. *Laser Phys. Lett.*, **6**, 487 (2009).
14. Razdobreev I., Bigot L., Pureur V., Favre A., Bouwmans G., Douay M. *Appl. Phys. Lett.*, **90**, 031103-1 (2007).
15. Kalita M.P., Yoo S., Sahu J. *Opt. Express*, **16**, 21032 (2008).
16. Dianov E.M., Dvoyrin V.V., Mashinsky V.M., Medvedkov O.I. *Proc. ECOC* (Cannes, 2006) paper Th.2.3.1.
17. Firstov S.V., Khopin V.F., Bufetov I.A., Firstova E.G., Guryanov A.N., Dianov E.M. *Opt. Express*, **19**, 19551 (2011).
18. Dianov E.M., Shubin A.V., Melkumov M.A., Medvedkov O.I., Bufetov I.A. *J. Opt. Soc. Am. B*, **24**, 1749 (2007).
19. Dvoyrin V.V., Mashinsky V.M., Dianov E.M. *IEEE J. Quantum Electron.*, **44**, 834 (2008).
20. Dvoyrin V.V., Kir'yanov A.V., Mashinsky V.M., Medvedkov O.I., Umnikov A.A., Guryanov A.N., Dianov E.M. *IEEE J. Quantum Electron.*, **46**, 182 (2010).
21. Dianov E.M., Krylov A.A., Dvoyrin V.V., Mashinsky V.M., Kryukov P.G., Okhotnikov O.G., Guina M. *J. Opt. Soc. Am. B*, **27**, 1807 (2007).
22. Kivistö S., Puustinen J., Guina M., Okhotnikov O.G., Dianov E.M. *Electron. Lett.*, **44**, 1456 (2008).
23. Krylov I.A., Kryukov P.G., Dianov E.M., Okhotnikov O.G. *Kvantovaya Elektron.*, **39**, 882 (2009) [*Quantum Electron.*, **39**, 882 (2009)].
24. Kivistö S., Gumenyuk R., Puustinen J., Guina M., Dianov E.M., Okhotnikov O.G. *IEEE Photonics Technol. Lett.*, **21**, 599 (2009).
25. Kivistö S., Puustinen J., Guina M., Herda R., Marcinkevicius S., Dianov E.M., Okhotnikov O.G. *Opt. Express*, **18**, 1041 (2010).
26. Luo A.-P., Luo Z.-C., Xu W.-C., Dvoyrin V.V., Mashinsky V.M., Dianov E.M. *Laser Phys. Lett.*, **8**, 601 (2011).
27. Bufetov I.A., Firstov S.V., Khopin V.F., Guryanov A.N., Dianov E.M. *Proc. ECOC* (Brussels, 2008) paper Tu.3.B.4.
28. Rulkov A.B., Ferin A.A., Popov S.V., Taylor J.R., Razdobreev I., Bigot L., Bouwmans G. *Opt. Express*, **15**, 5473 (2007).
29. Sadick N.S., Weiss R. *J. Dermatol. Surg.*, **28**, 21 (2002).
30. Blodi C.F., Russel S.R., Padilo J.S., Folk J.C. *Ophthalmology*, **6**, 791 (1990).
31. Max C.E., Olivier S.S., Friedman H.W., et al. *Science*, **277**, 1649 (1977).
32. Dvoyrin V.V., Mashinsky V.M., Dianov E.M. *Opt. Lett.*, **32**, 451 (2007).
33. Yoo S., Kalita M.P., Sahu J., Nilsson J., Oton C. *Proc. 3rd EPS-QEOD Europhoton Conf.* (Paris, 2008) paper THoE.5.
34. Dianov E.M., Mel'kumov M.A., Shubin A.V., Firstov S.V., Khopin V.F., Gur'yanov A.N., Bufetov I.A. *Kvantovaya Elektron.*, **39**, 1099 (2009) [*Quantum Electron.*, **39**, 1099 (2009)].
35. Bufetov I.A., Melkumov M.A., Khopin V.F., Firstov S.V., Shubin A.V., Medvedkov O.I., Guryanov A.N., Dianov E.M. *Proc. SPIE Int. Soc. Opt. Eng.*, **7580**, 758014-1 (2010).
36. Bufetov I.A., Shubin A.V., Firstov S.V., Melkumov M.A., Khopin V.F., Guryanov A.N., Dianov E.M. *Proc. CLEO/Europe-EQEC Conf.* (Munich, 2011) paper cJ 8.2.
37. Dianov E.M., Bufetov I.A., Firstov S.V., Medvedkov O.I., Melkumov M.A. *Proc. ECOC* (Geneva, 2011) paper Tu 3, Le Cervin 3.
38. Firstov S.V., Shubin A.V., Khopin V.F., Mel'kumov M.A., Bufetov I.A., Medvedkov O.I., Gur'yanov A.N., Dianov E.M. *Kvantovaya Elektron.*, **41**, 581 (2011) [*Quantum Electron.*, **41**, 581 (2011)].
39. Shubin A.V., Bufetov I.A., Melkumov M.A., Firstov S.V., Medvedkov O.I., Khopin V.F., Guryanov A.N., Dianov E.M. *Opt. Lett.*, **37**, 2589 (2012).
40. Melkumov M.A., Bufetov I.A., Shubin A.V., Firstov S.V., Khopin V.F., Guryanov A.N., Dianov E.M. *Opt. Lett.*, **36**, 2408 (2011).

41. Bufetov I.A., Melkumov M.A., Firstov S.V., Shubin A.V., Semenov S.L., Vel'miskin V.V., Levchenko A.E., Firstova E.G., Dianov E.M. *Opt. Lett*., **36**, 166 (2011).
42. Krasnovsky A.A., Drozdova N.N., Ivanov A.V., Ambartsumian R.V. *Biochemistry (Moscow),* **68**, 963 (2003).
43. Corbett J.D. *Prog. Inorg. Chem*., **21**, 129 (1976).
44. Khonton S., Morimoto Sh., Arai Y., Ohishi Y. *Opt. Mater.*, **31**, 1262 (2009).
45. Dianov E.M. *Kvantovaya Elektron*., **40**, 283 (2010) [*Quantum Electron*., **40**, 283 (2010)].
46. Razdobreev I., El Hamzaoui H., Ivanov V.Yu., Kustov E.F., Capoen B., Bouazaoui M. *Opt. Lett*., **35**, 1341 (2010).